

1 **Boosting Lewis Acidic Sites via SMSI to Enriched Oxygen Vacancy**  
2 **on Pt-CeO<sub>2</sub> Catalysts Enhancing Efficiency of CO Promoted Toluene**  
3 **Catalysis**

4  
5 Xiaoying Zhou <sup>a</sup>, Mingyuan Zhang <sup>a, \*</sup>, Peiqi Mao <sup>a</sup>, Jiaxuan Pang <sup>a</sup>, Jiayi Wang <sup>b</sup>, Liping Wang <sup>a</sup>,  
6 Chentao Hou <sup>a, \*</sup>, Daiqi Ye <sup>c, \*</sup>

7  
8 <sup>a</sup> School of Geology and Environment, Xi'an University of Science and Technology, Xi'an 710054,  
9 China.

10 <sup>b</sup> Non-metallic Mine Research and Design Institute Co., Ltd, Xianyang 712000, China.

11 <sup>c</sup> School of Environment and Energy, South China University of Technology, Guangzhou 510006,  
12 China.

13 \*Corresponding Author: zhangmy@xust.edu.cn (M. Zhang), houct@xust.edu.cn (C. Hou),  
14 cedqye@scut.edu.cn (Q. Ye).

15

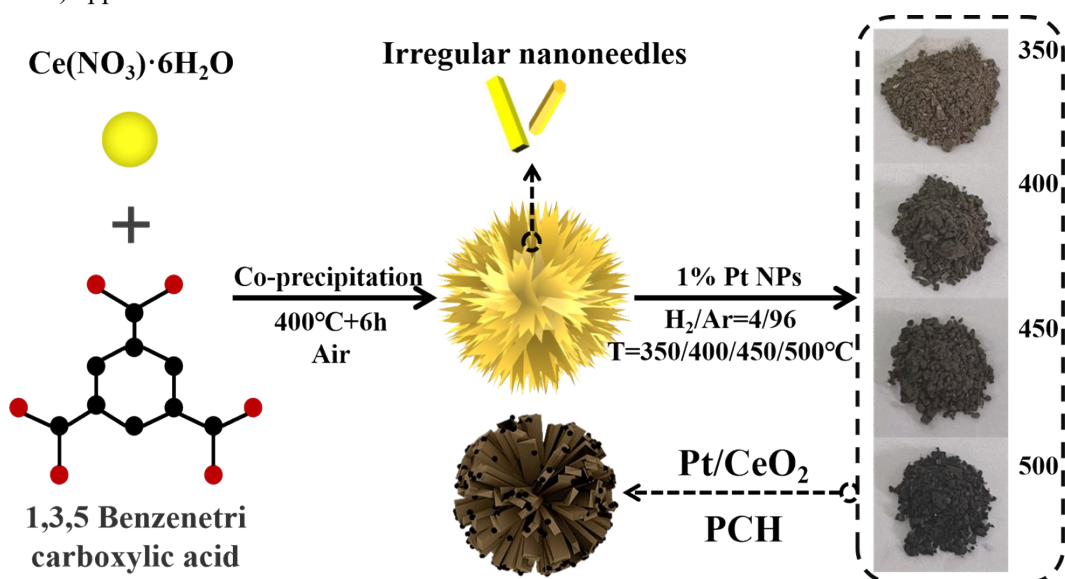
16

17

# 1 Experiment

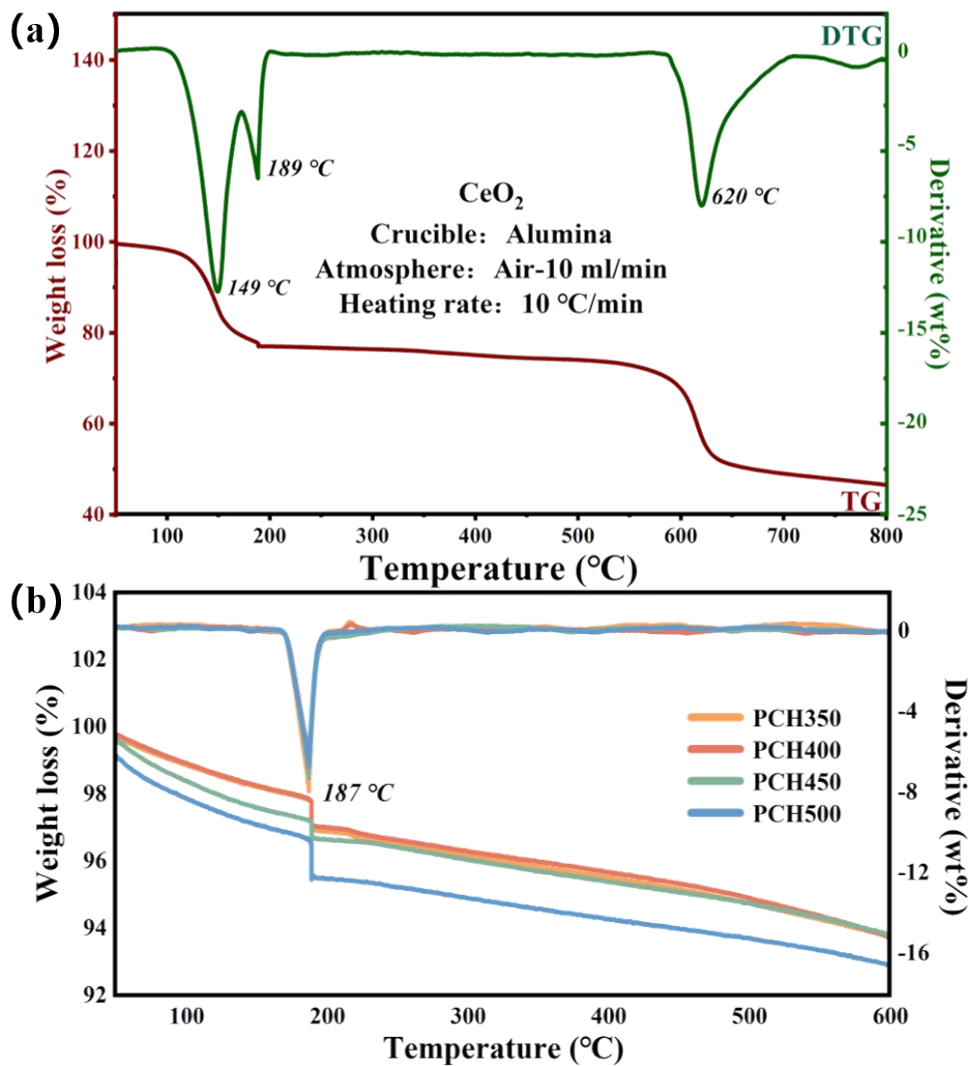
## 2 2.2 Characterization of catalysts

3 In this work, the crystal structure and quality of the nanomaterials were determined using X-ray  
4 powder diffraction (XRD, D8 ADVANCE, Bruker-AXS, Germany). The specific surface area of  
5 the nanomaterials was measured using the BET method in a nitrogen atmosphere with a fully  
6 automatic surface analyzer (ASAP 2020M, Micromeritics, USA). The morphologies of different  
7 catalyst samples were observed using scanning electron microscopy (SEM, Merli, Panaco,  
8 Netherlands). The microstructure of all samples was examined using transmission electron  
9 microscopy (TEM, JEM-2010F, JEOL, Japan). H<sub>2</sub>-temperature programmed reduction, O<sub>2</sub>-  
10 temperature programmed desorption, and NH<sub>3</sub>-temperature programmed desorption experiments  
11 were conducted on various catalysts using BSD-Chem C200 (Beishide Instrument Technology,  
12 Beijing). These experiments aimed to investigate the reducibility of the nanomaterials and the  
13 relationship between the oxygen species and acidic sites on the catalyst surface. The surface defect  
14 structure and oxygen vacancy content of different samples were measured using visible/UV-  
15 Raman spectroscopy with a LabRAM HR Evolution Laser (HYJ, France). In situ tracking and  
16 detection of intermediate species adsorbed on the catalyst surface during the catalytic reaction  
17 were performed using Fourier infrared spectroscopy (INVENIO-S, Bruker, Germany). The Pt  
18 content on all catalyst surfaces was quantified using an iCAP 6300 inductively coupled plasma  
19 emission spectrometer (PerkinElmer, USA). The densities of Bronsted and Lewis acids were  
20 determined by the pyridine adsorption infrared (Py-IR) method with the Nicolet-380 (Bruker  
21 tensor27) apparatus.



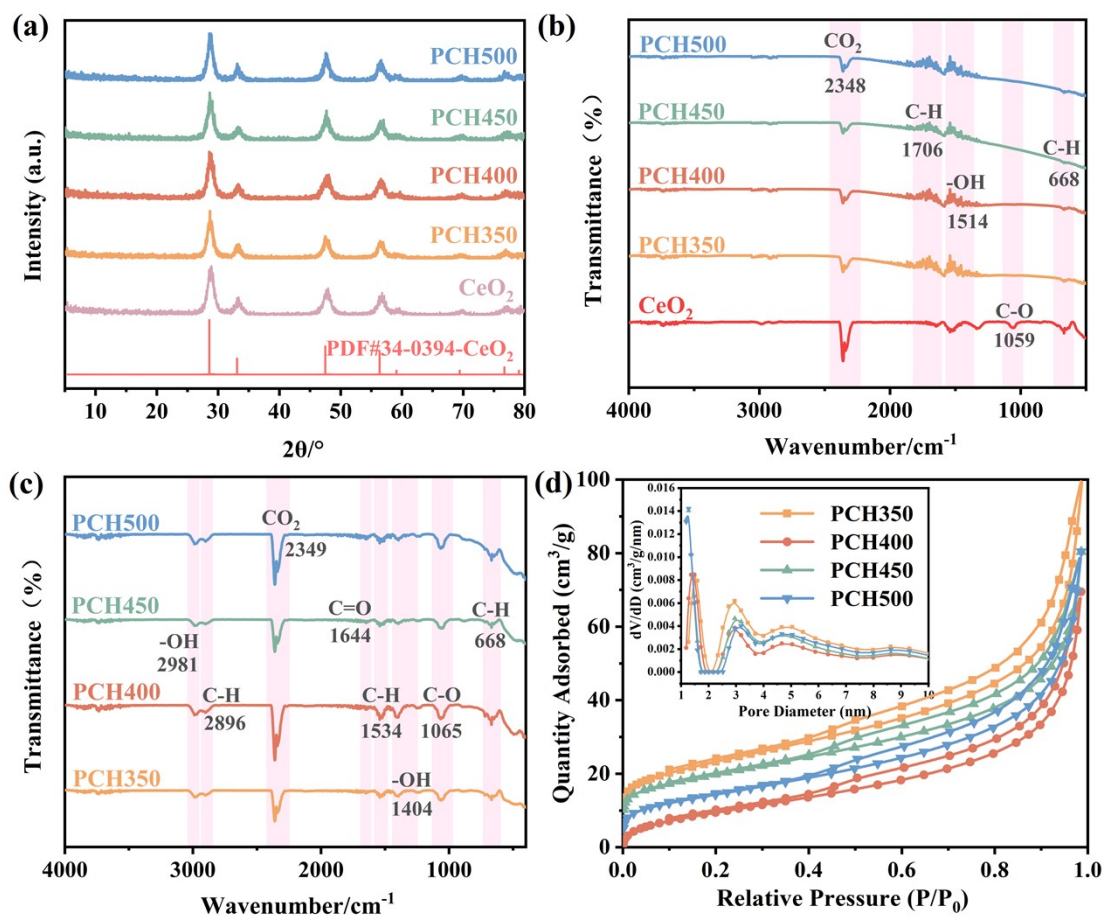
22

23 **Fig. S1.** Schematic diagram of preparation of PCH catalytics.

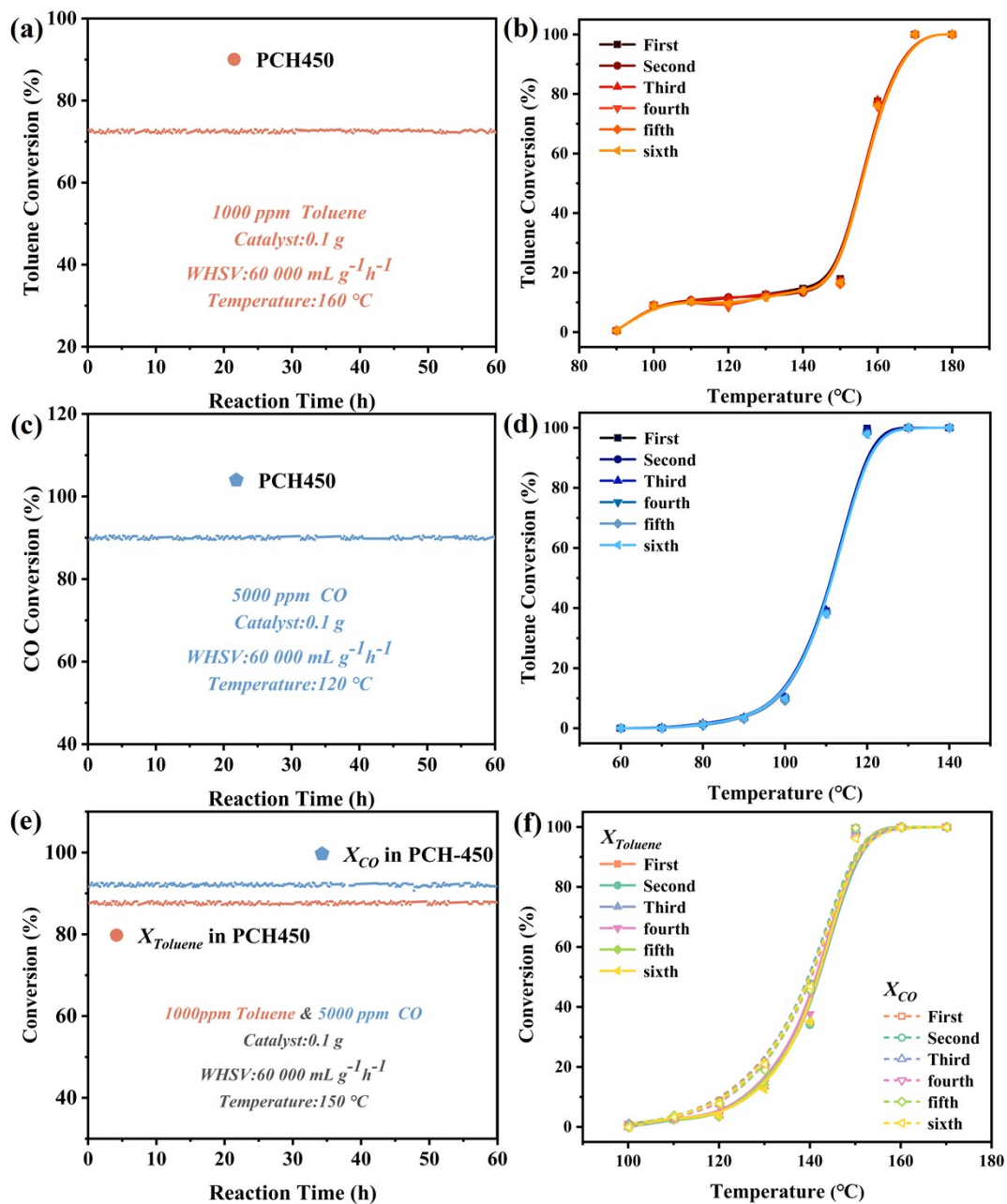


1

2 **Fig. S2.** Curves of TGA over (a)  $\text{CeO}_2$ ; (b) PCH catalytics.



1  
 2 **Fig. S3.** (a) XRD patterns of PCH catalysts after reaction; FT-IR spectra of (b) Before reaction, (c)  
 3 After reaction on PCH catalysts; (d) BET of PCH catalysts.

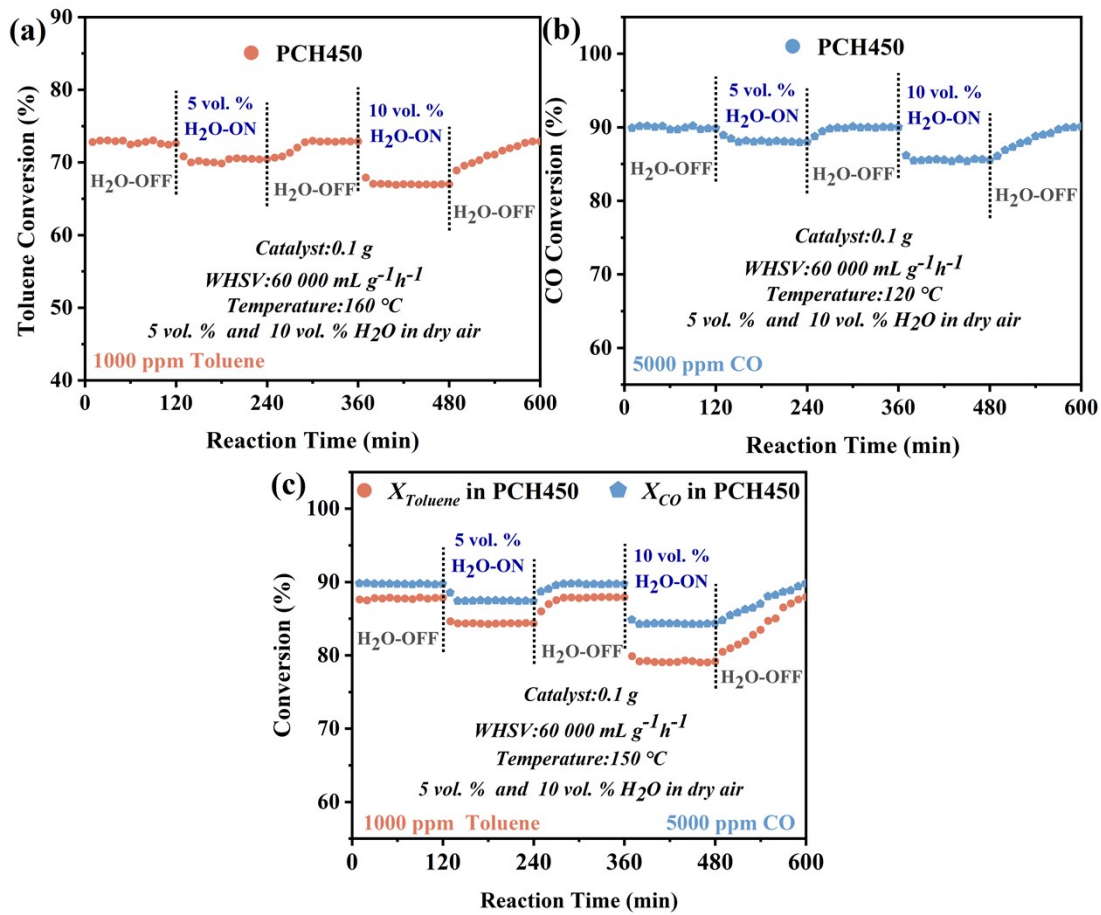


1

2 **Fig. S4.** Tests of durability for (a) Toluene, (c) CO, and (e) Toluene + CO conversion on PCH450  
 3 catalyst. Tests of multiple cyclicality for (a) Toluene, (c) CO, and (e) Toluene + CO conversion on  
 4 PCH450 catalyst.

5

6



1

2 **Fig. S5.** Tests of resistance to water vapor interference for (b) Toluene, (d) CO, and (f) Toluene +  
 3 CO conversion on PCH450 catalyst.